EUROPEAN ORGANIZATION FOR NUCLEAR RESEARCH

CERN-EP/87-22
10 February 1987

STUDY OF THE REACTION $\bar{p}p \to \bar{\Lambda}\Lambda$ NEAR THRESHOLD

P.D. Barnes[1], R. Besold[3,a], P. Birien[6,b], B. Bonner[5,c], W.H. Breunlich[8], W. Dutty[4], R.A. Eisenstein[1,d], G. Ericsson[7], W. Eyrich[3], R. von Frankenberg[3], G. Franklin[1], J. Franz[4], N. Hamann[4], D. Hertzog[1,d], A. Hofmann[3], T. Johansson[7], K. Kilian[2,e], C.J. Maher[1,f], S. Ohlsson[7], H. Ortner[3], P. Pawlek[8], B. Quinn[1], E. Rössle[4], H. Schledermann[4], H. Schmitt[4] and W. Wharton[1,g]

1) Carnegie-Mellon University, Pittsburgh, PA 15213, USA.
2) CERN, 1211 Geneva 23, Switzerland.
3) University of Erlangen-Nuremberg, 8520 Erlangen, Fed. Rep. Germany.
4) University of Freiburg, 7800 Freiburg, Fed. Rep. Germany.
5) Los Alamos Nat. Laboratory, Los Alamos, NM 87545, USA.
6) DPhN, CEN-Saclay, 91191 Gif-sur-Yvette, France.
7) University of Uppsala, 75121 Uppsala, Sweden.
8) Österreich. Akad. Wissensch., 1090 Vienna, Austria.

ABSTRACT

Results are presented from a study of the reaction $\bar{p}p \to \bar{\Lambda}\Lambda$ near threshold. Over 3000 events recorded at $\sqrt{s}$ values of 14.6 and 25.5 MeV above the $\bar{\Lambda}\Lambda$ threshold (2231.2 MeV) have been analysed. Results for the production cross-section, differential cross-section, and the $\bar{\Lambda}$ and Λ polarization are given at both energies and are compared with recent theoretical calculations of this process.

(Submitted to Physics Letters B)

Present addresses:
a) Siemens AG, 8500 Nuremberg, Fed. Rep. Germany.
b) Univ. of Freiburg, 7800 Freiburg, Fed. Rep. Germany.
c) Rice Univ., Houston, TX 77251, USA.
d) Univ. of Illinois, Champaign, IL 61820, USA.
e) Kernforschungsanlage Jülich, 5170 Jülich, Fed. Rep. Germany.
f) Massachusetts Inst. of Technology, Cambridge, MA 02139, USA.
g) Wheaton Coll., Wheaton, IL 60187, USA.

The reaction $\bar{p}p \to \bar{\Lambda}\Lambda$ provides an especially attractive process in which to investigate the creation of strange quarks. In earlier bubble-chamber experiments [1-3], the reaction has been studied up to 6 GeV/c incident $\bar{p}$ momentum. In addition to cross-section measurements, the self-analysing character of the $\bar{\Lambda}$ and Λ weak decays [4] can provide information on the spin variables in the final state, without the need to perform a double-scattering experiment. We report the first results from an ongoing study [5] (CERN experiment PS185) of antihyperon-hyperon ($\bar{\Lambda}\Lambda$, $\bar{\Lambda}\Sigma + \bar{\Sigma}\Lambda$, $\bar{\Sigma}\Sigma$) creation in $\bar{p}p$ collisions. The production cross-sections, differential cross-sections, final-state polarization, and spin-correlation coefficients are studied near threshold. An intriguing feature of associated strangeness production is the similarity of Λ polarizations in different reactions [5]. This might be due to the fact that, in the additive quark model, the Λ hyperon is composed of an s quark coupled to a spin- and isospin-zero ud quark pair. Therefore the reaction $\bar{p}p \to \bar{\Lambda}\Lambda$ allows one to relate the final-state spin effects to the quantum numbers of the $\bar{s}s$ creation vertex.

Several models for $\bar{p}p \to \bar{\Lambda}\Lambda$ have been suggested. This reaction might be viewed as a t-channel exchange of K(494 MeV;0^-), K^*(892 MeV;1^-), and even K_2^*(1430 MeV;2^+) and K_0^*(1350 MeV;0^+) mesons (see Fig. 1a). Meson-exchange calculations of cross-sections and of final-state spin variables have been made recently by several groups [6-10]. These calculations indicate that the cross-section and the polarization are sensitive to the transition potential, to $\bar{p}p$ initial-state interactions, and to the less well-known $\bar{\Lambda}\Lambda$ final-state interactions. The models differ widely in the relative importance of the exchanged kaons. The exchange of strange mesons in the t-channel corresponds to the $\bar{u}u$ quark-pair annihilation and $\bar{s}s$ creation in the direct channel (see Fig. 1b). A perturbative QCD calculation would not seem to be valid at low energies, yet some dynamics of the effective strange-quark production can be learned in this framework [11-13]. Models have been adopted

in which the $\bar{s}s$ creation vertex has the quantum numbers of a gluon ($^3S_1$ model) or those of the vacuum ($^3P_0$ model).

The data reported here were obtained at the CERN Low Energy Antiproton Ring (LEAR). The incident $\bar{p}$ momenta were 1476.5 MeV/c and 1507.5 MeV/c, corresponding to centre-of-mass energies above threshold, $\varepsilon = \sqrt{s} - 2231.2$ MeV, of 14.6 and 25.5 MeV, respectively. The $\bar{p}$ flux varied from 1.0 to 1.5 x 10^5 s^{-1} over one-hour beam-extraction times. The total number of $\bar{p}$'s obtained at the two momenta was 2.3 x 10^{10} and 1.9 x 10^{10}. The spot size of the focused beam was measured with a scintillation scanning device to be 1.25 mm horizontally and 0.5 mm vertically (FWHM) at the location of the interaction target.

The $\bar{\Lambda}\Lambda$ pairs recoil downstream within a narrow cone of 10.0° and 13.1° for the two incident beam momenta studied. The hyperon momenta range from 550 to 960 MeV/c, corresponding to average decay lengths between 3.9 and 6.8 cm. In 41.2% of the cases both decays produce charged particles ($\Lambda \rightarrow p\pi^-$, $\bar{\Lambda} \rightarrow \bar{p}\pi^+$), where most of the momentum is carried downstream by the secondary proton and antiproton. For both, the laboratory angle is limited to 19.5° and 22.6°, respectively, for the two incident momenta. A stack of wire chambers records the distinctive two-vertex signature of a $\bar{\Lambda}\Lambda$ decay into four charged particles with a 4π centre-of-mass acceptance for the secondary proton and antiproton. These events can be reconstructed entirely from the geometric features of their tracks and the kinematics of the reaction, without the need for momentum analysis in a magnetic field.

A plan view of the detector with an overlay of an identified $\bar{p}p \rightarrow \bar{\Lambda}\Lambda$ event is shown in Fig. 2. The antiproton beam impinges on a 2.7 mm long by 2.5 mm diameter CH_2 target, which is housed in a segmented cylindrical veto scintillator enclosure (S2). A pair of 0.1 mm thick scintillators (S1A and S1B) are used to define the arrival of an antiproton. A 0.1 mm thick veto scintillator (S3) is placed at the exit of the target (see Frankenberg et al. [14] for details). Thus a neutral target event is defined as $S1A \cdot S1B \cdot \overline{S2} \cdot \overline{S3}$.

The decay proton and antiproton pass through two 22-element, 4 mm thick, plastic scintillation hodoscopes (H_x and H_y) positioned 63 cm downstream of the target. A signal of one or more hits in each hodoscope plane is used in coincidence with the neutral target event to identify the 'charged-neutral-charged' signature of a candidate event. The stack of wire chambers consists of a 10-plane multiwire proportional chamber stack (MWPC) and a 12-plane drift chamber stack. The wires of the MWPC planes are oriented alternately at $\pm 45^\circ$ with respect to the horizontal, and each plane consists of 160 wires spaced 1.27 mm apart. The drift chamber wires are oriented horizontally (x) and vertically (y). Each plane contains 14 drift cells of 4 cm width. They are read out by a pair of sense wires separated by 0.4 mm. A typical drift-chamber resolution of 0.2 mm is achieved for small-angle tracks. In both sets of chambers the central wires are made insensitive over a few mm to allow the non-interacting $\bar{p}$ beam to pass without buildup of space charge and to avoid dead-time losses for real events on the central wires (see Dutty et al. [15] for details). The decay products passing through the hodoscope enter a solenoid with a 0.1 T vertical magnetic field. Three drift chambers inside the solenoid serve to distinguish the baryon number (± 1) of the two identified vertices through sign measurement of the particle charges. The data were digitized in CAMAC modules and transferred by a micro-programmable branch driver to a VAX 11/750 for monitoring and writing on magnetic tape (see Maher [16] for details).

The analysis for $\bar{\Lambda}\Lambda$ candidate events included three-dimensional track fitting to chamber hits, a vertex candidate search, and full kinematic fitting of pairs of matched vertices assuming an event type $\bar{p}p \to \bar{\Lambda}\Lambda \to \bar{p}\pi^+ p\pi^-$. A $\bar{\Lambda}\Lambda$ event was defined as one in which the reduced χ^2 fell below 5. Sources of two-vertex background arise from $\bar{p}p \to K_S K_S X$ events or $\bar{\Lambda}\Lambda$ production on carbon. The kinematics of $K_S K_S X$ events are very different from $\bar{\Lambda}\Lambda$ production and do not have low χ^2 when fitted to the $\bar{p}p \to \bar{\Lambda}\Lambda$ hypothesis. A background

run at 1476.5 MeV/c was made using a pure carbon target. Events from this run which survived the above $\bar{p}p \to \bar{\Lambda}\Lambda$ assumption represented a contribution from the carbon in the CH_2 target of less than 1.5% in the main data sample. The deflection in the solenoid was used to identify $\bar{\Lambda}$ and Λ in the reconstructed events. In about 85% of the cases, a clear distinction existed, and only these events were included in the final angular distributions discussed below.

In order to obtain the differential cross-section, the uncorrected $\cos \theta^*_{\bar{\Lambda}}$ angular distribution was extracted from the data and was corrected by an acceptance curve generated from a Monte Carlo simulation. A great effort was made to model the actual performance of the detector system by including effects such as the small beam-axis dead spots on the chambers, occasional uncorrelated hits in the chambers, and chamber-plane efficiencies. Simulated events were generated with isotropic centre-of-mass angular distribution and without polarization of the outgoing $\bar{\Lambda}\Lambda$ pairs. They were analysed using the same algorithm and cuts described for the analysis of the actual data, giving the angular dependence of the detector acceptance function. The efficiency of baryon-number identification was found to be angle-independent and could be folded into the overall detector efficiency determined from the Monte Carlo simulations.

The measured production cross-sections and their statistical errors are listed in Table 1. Systematic errors are estimated to be of the order of 10%. A comparison with previous measurements is included in Table 1. The differential cross-sections in the centre of mass are shown in Fig. 3a and b. The hyperon polarization can be explored using the weak decays $\bar{\Lambda} \to \bar{p}\pi^+$ and $\Lambda \to p\pi^-$. In the rest frame of the hyperon, the outgoing nucleon is preferentially emitted along the Λ spin direction, yielding the distribution $I(\theta_p) = I_0(1 + \alpha P \cos \theta_p)$ for a sample with polarization P. The angle θ_p is measured between the normal to the reaction plane and the nucleon momentum in

the Λ rest frame, and $\alpha = 0.642 \pm 0.013$ is the $\Lambda \to p\pi^-$ decay asymmetry parameter. The polarization has been evaluated for five equal $\cos\theta^*_{\bar{\Lambda}}$ bins for $\bar{\Lambda}$ and Λ separately, taking into account the acceptance function for the decay particles. The results are shown in Fig. 3c and d. The polarization in the $\bar{\Lambda}\Lambda$ production plane was measured [16] to be consistent with zero, as expected from parity conservation in strong interactions. There were not enough events in the present measurement to extract accurate spin-correlation coefficients. This has to await the analysis of more data.

In the absence of distortions, the ratio of $\bar{\Lambda}\Lambda$ production cross-sections, $R = \sigma_{\bar{\Lambda}\Lambda}(1507.5\ \mathrm{MeV/c})/\sigma_{\bar{\Lambda}\Lambda}(1476.5\ \mathrm{MeV/c})$, is expected to be 1.32 for pure S-wave and 2.31 for pure P-wave production. Our measured value $R = 1.93 \pm 0.13$ suggests strong contributions from partial waves with $l > 0$, or the presence of distortions, at these momenta. Clear evidence for $l > 0$ contributions comes from the strong anisotropy of the differential cross-sections in Fig. 3. As shown in Fig. 4a, the forward peak as well as the general magnitude of the cross-section at these momenta is reproduced by recent calculations [6, 9] despite the fact that the various models involved are based on rather different assumptions. For the polarization data shown in Fig. 3, there is good agreement between the $\bar{\Lambda}$ and the Λ distributions as expected from charge-conjugation invariance. The 1507.5 MeV/c data indicate that the polarization is positive at angles forward of $\cos\theta^*_{\bar{\Lambda}} = 0.2$ [squared four-momentum transfer $t\text{-}t_{min} = -0.17\ (\mathrm{GeV/c})^2$] and negative at larger angles. As shown in Fig. 4b, both the one-kaon and the one-gluon exchange calculations by Kohno and Weise give a polarization distribution similar to the data, whereas the calculation by Tabakin and Eisenstein predicts no change in sign. More data on polarization and spin-correlation parameters, and perhaps improved calculations, may provide a basis for a more detailed comparison between experiment and theory.

We wish to thank the LEAR accelerator team for the development and excellent operation of the antiproton beams required for these experiments. We acknowledge support from the Austrian Science Foundation, the German Bundesministerium für Forschung und Technologie, the Swedish Natural Science Research Council, and the United States Department of Energy. This work is based in part on a dissertation submitted by one of us (C.J.M) to the Carnegie-Mellon University in partial fulfilment of the requirements for the Ph.D. degree.

REFERENCES

[1] B. Jayet et al., Nuovo Cimento 45A (1978) 371.

[2] B.Y. Oh et al., Nucl. Phys. B51 (1973) 57.

[3] H.W. Atherton et al., Nucl. Phys. B69 (1974) 1;
N. Kwak et al., Nuovo Cimento 23A (1974) 610;
H. Becker et al., Nucl. Phys. B141 (1978) 48.

[4] L. Durand and J. Sandweiss, Phys. Rev. 135 (1964) B540.

[5] K. Kilian, CERN/PSCC/81-29/I59 (1981);
PS185 Collaboration, CERN/PSCC/81-69/P49 (1981).

[6] F. Tabakin and R.A. Eisenstein, Phys. Rev. C31 (1985) 1857.

[7] M. Dillig and R. von Frankenberg, Proc. Int. Conf. on Antinucleon- and Nucleon-Nucleus Interactions, Telluride, 1985, eds. G.E. Walker et al. (Plenum Press, New York, 1985), p. 399.

[8] J.A. Niskanen, Helsinki Univ. preprint HU-TFT-85-28 (1985);
A.M. Green and J.A. Niskanen, Helsinki Univ. preprint HU-TFT-85-60 (1985).

[9] M. Kohno and W. Weise, Phys. Lett. 179B (1986) 15.

[10] J.J. DeSwart et al., Nijmegen Univ. preprint THEF-NYM-86.03 (1986).

[11] H. Genz and S. Tatur, Phys. Rev. D30 (1984) 63.

[12] H.R. Rubinstein and H. Snellman, Phys. Lett. 165B (1985) 187.

[13] S. Furui and A. Faessler, Tübingen Univ. preprint (Dec. 1986).

[14] R. von Frankenberg et al., Nucl. Instrum. Methods A243 (1986) 98.

[15] W. Dutty et al., Nucl. Instrum. Methods A252 (1986) 570.

[16] C.J. Maher, Ph.D. Thesis, Physics Department, Carnegie-Mellon Univ. (1986), unpublished.

Table 1

Cross-section summary

$\bar{p}$ momentum (MeV/c)	ε (MeV)	$\bar{\Lambda}\Lambda$ events	$\sigma_{\bar{\Lambda}\Lambda}$ (μb)	Reference
1476.5 $\pm$ 1.8	14.6 $\pm$ 0.6	1185	13.8 $\pm$ 0.5	This work
1507.5 $\pm$ 1.8	25.5 $\pm$ 0.6	1845	26.6 $\pm$ 0.7	This work
1500 $\pm$ 15	23 $\pm$ 5	18	24.6 $\pm$ 5.9	Ref. [1]
1510	26	$\approx$ 25	58 $\pm$ 14	Ref. [2]

Figure captions

Fig. 1: The reaction $\bar{p}p \to \bar{\Lambda}\Lambda$, viewed (a) as a t-channel meson exchange, and (b) as a $\bar{u}u$ quark-pair annihilation and $\bar{s}s$ creation process.

Fig. 2: Experimental set-up with: 1 = target region (see magnified view), 2 = multiwire proportional chambers, 3 = drift chambers, 4 = scintillator hodoscope, and 5 = magnetic solenoid with drift chambers.

Fig. 3: Results (a,b) for the differential cross-sections, and (c,d) for the polarization distributions (open circles: $\bar{\Lambda}$ polarization, full circles: Λ polarization) at 1476.5 and 1507.5 MeV/c.

Fig. 4: Comparison (a) of the differential cross-section data, and (b) of the polarization data (averaged over the $\bar{\Lambda}$ and Λ polarization) at 1507.5 MeV/c with the meson-exchange calculations by Kohno and Weise [9] (solid) and by Tabakin and Eisenstein [6] (dash-dotted), and with the gluon-exchange calculation by Kohno and Weise [9] (dashed).

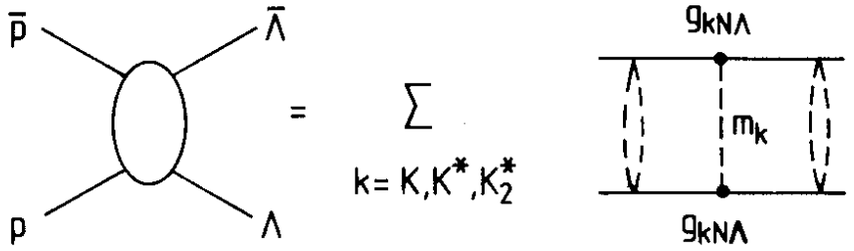

(a)

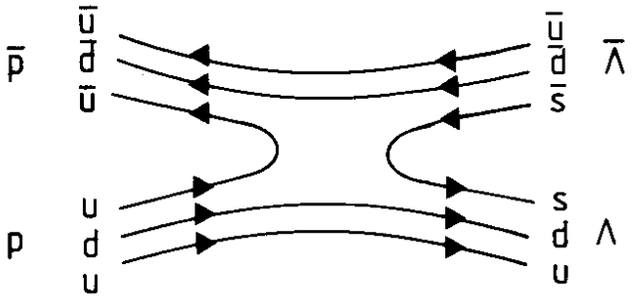

(b)

Fig. 1

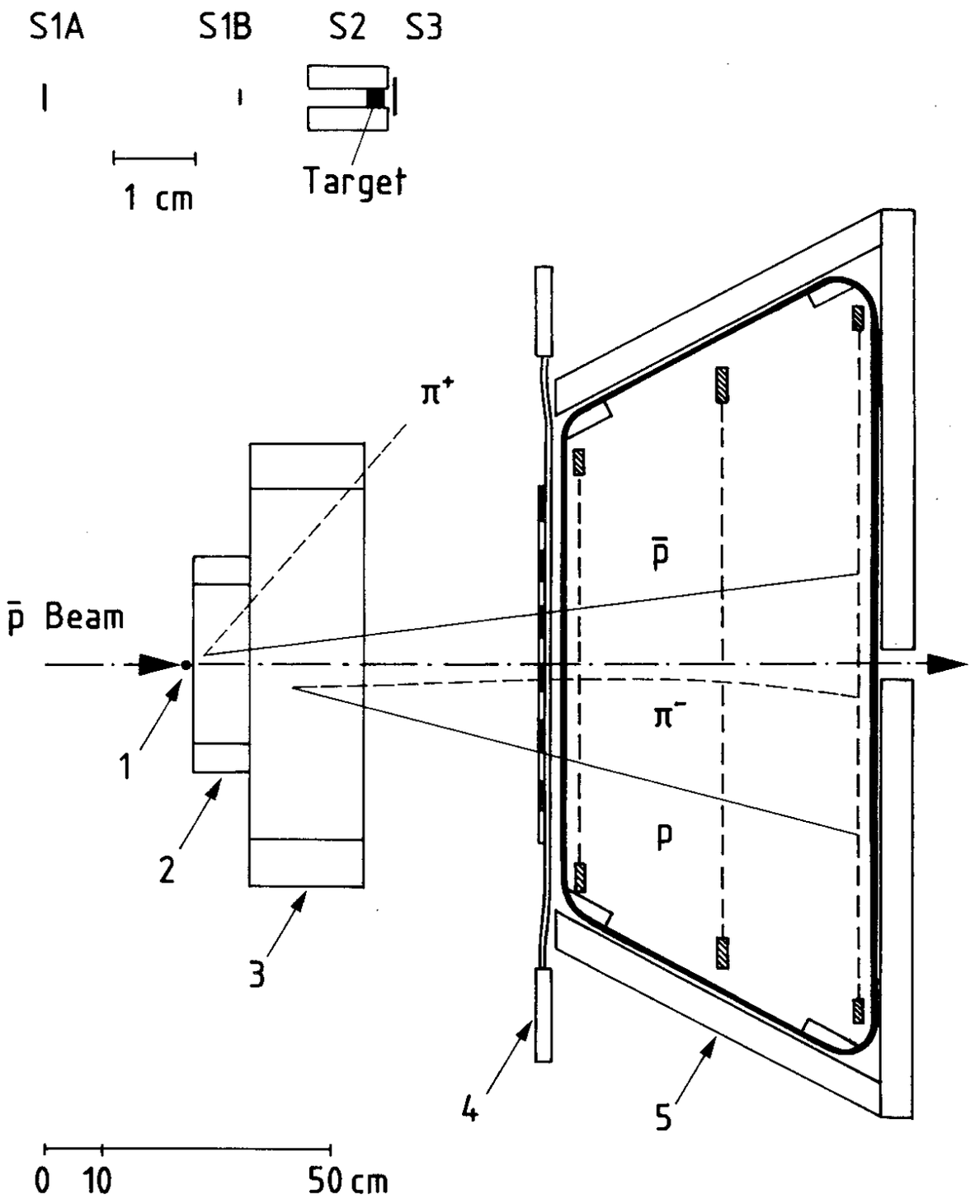

Fig. 2

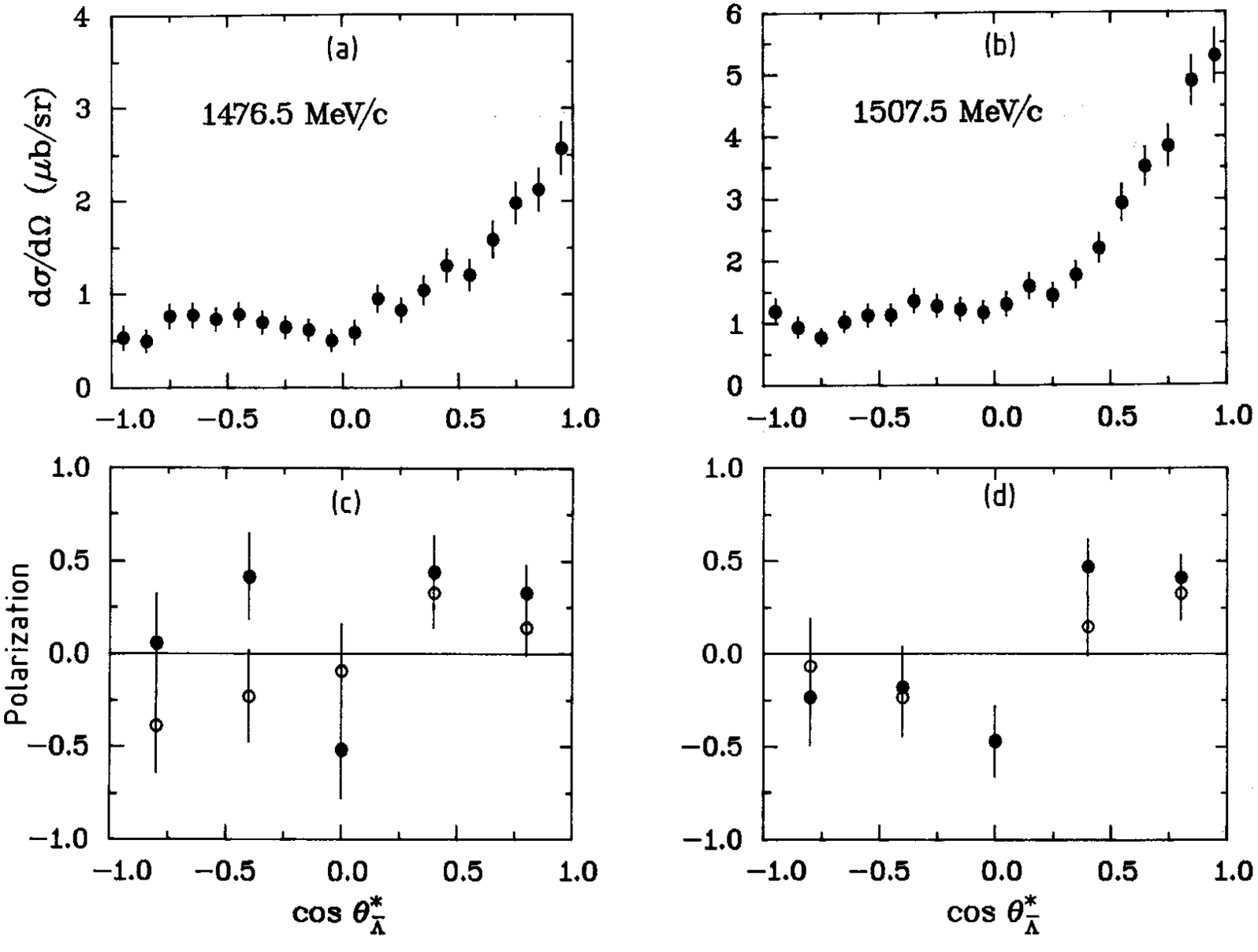
(a)
1476.5 MeV/c
(b)
1507.5 MeV/c
(c)
(d)
dσ/dΩ (μb/sr)
Polarization
cos θ*Λ
cos θ*Λ

Fig. 3

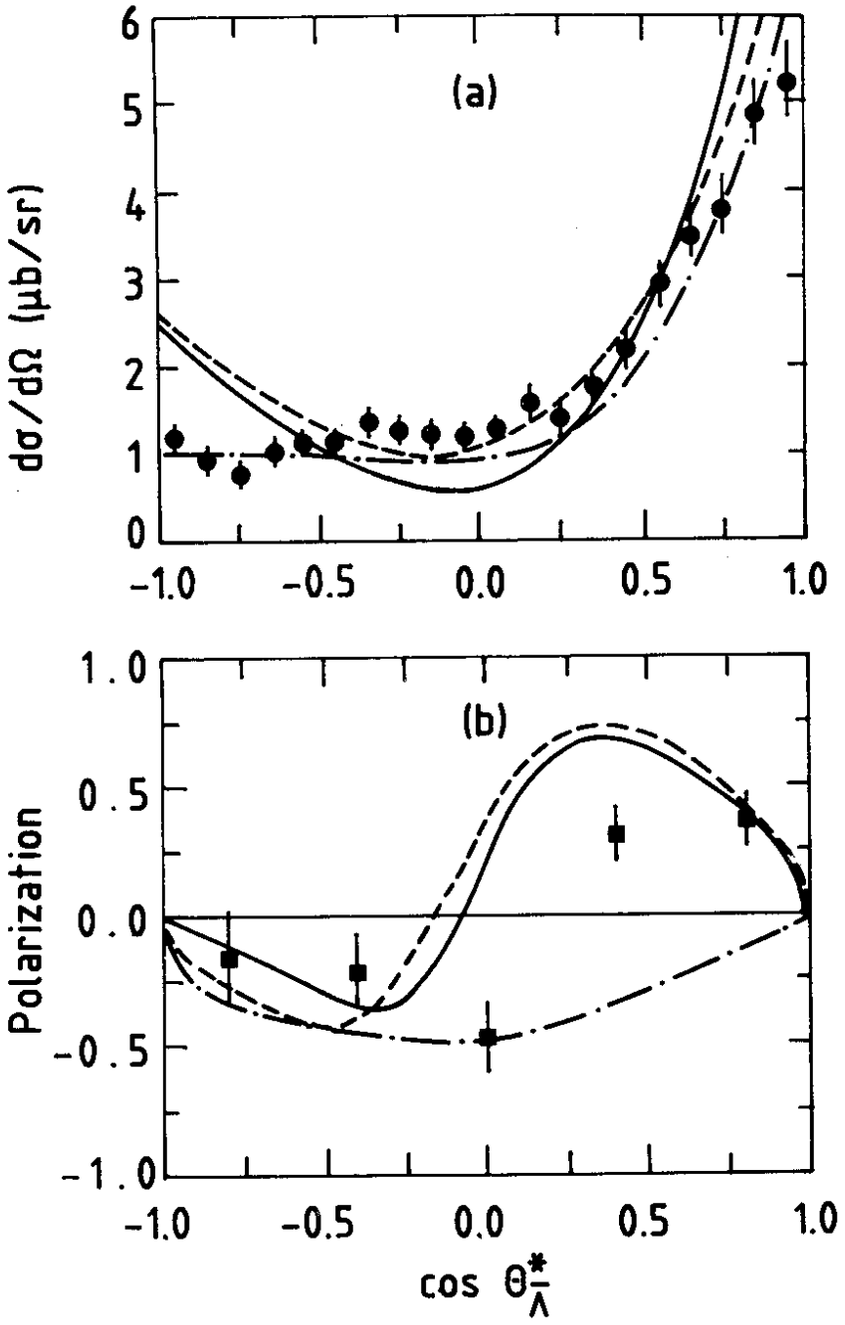
(a)
dσ/dΩ (μb/sr)
6
5
4
3
2
1
0
-1.0
-0.5
0.0
0.5
1.0
(b)
Polarization
1.0
0.5
0.0
-0.5
-1.0
cos θ*Λ

Fig. 4